

# 一个新的三维配位聚合物 $\text{Na}[\text{Cu}_2(\text{malonate})_2] \cdot (\text{ClO}_4) \cdot (\text{H}_2\text{O})_2$ 的合成与表征

陈 军<sup>1,2</sup> 张 中<sup>1</sup> 徐 伟<sup>1</sup> 宋 友<sup>1</sup> 王志林<sup>\*,1</sup>

(<sup>1</sup> 南京大学配位化学研究所, 配位化学国家重点实验室, 南京 210093)

(<sup>2</sup> 淮海工学院化学工程系, 连云港 222005)

**摘要:** 通过  $\text{Cu}(\text{ClO}_4)_2$  和丙二酸在水溶液中的自组装合成了一个新的 3D 配位聚合物  $\text{Na}[\text{Cu}_2(\text{malonate})_2] \cdot (\text{ClO}_4) \cdot (\text{H}_2\text{O})_2$ 。X-射线结构分析表明该化合物晶体属于正交晶系 *Pnma* 空间群( $a=1.256\ 5(3)$ ,  $b=1.059\ 4(2)$ ,  $c=1.075\ 5(14)$  nm,  $V=1.431\ 7(4)$  nm<sup>3</sup>,  $Z=4$ )。该聚合物的空间堆积在沿 *b* 轴和 *c* 轴方向分别形成大小为  $0.98\text{ nm} \times 0.83\text{ nm}$  和  $0.40\text{ nm} \times 0.40\text{ nm}$  的方形孔洞, 在沿 *a* 轴方向形成大小为  $0.85\text{ nm} \times 0.40\text{ nm}$  的砖墙形孔洞。磁性测试结果表明该化合物显示出铁磁性。导电性能测试实验表明它是一个半导体, 经拟合得到其活化能为  $0.80\text{ eV}$ 。

**关键词:** 铜; 丙二酸; 配位聚合物; 自组装; 半导体; 铁磁性

中国分类号: O614.112; O614.121

文献标识码: A

文章编号: 1001-4861(2005)05-0679-06

## Synthesis and Characterization of a New 3D Polymer $\text{Na}[\text{Cu}_2(\text{malonate})_2] \cdot (\text{ClO}_4) \cdot (\text{H}_2\text{O})_2$

CHEN Jun<sup>1,2</sup> ZHANG Zhong<sup>1</sup> XU Wei<sup>1</sup> SONG You<sup>1</sup> WANG Zhi-Lin<sup>\*,1</sup>

(<sup>1</sup> Coordination Chemistry Institute, The State Key Laboratory of Coordination Chemistry, Nanjing University, Nanjing 210093)

(<sup>2</sup> Department of Chemical Engineering, Huaihai Institute of Technology, Lianyungang 222005)

**Abstract:** A new 3D polymer,  $\text{Na}[\text{Cu}_2(\text{malonate})_2] \cdot (\text{ClO}_4) \cdot (\text{H}_2\text{O})_2$  was synthesized through the self-assembly of  $\text{Cu}(\text{ClO}_4)_2$  and malonic acid in aqueous solution and characterized by X-ray structure analysis. The compound crystallizes in Orthorhombic, space group *Pnma* ( $a=1.256\ 5(3)$ ,  $b=1.059\ 4(2)$ ,  $c=1.075\ 5(14)$  nm,  $V=1.431\ 7(4)$  nm<sup>3</sup>,  $Z=4$ ) and shows novel  $0.98\text{ nm} \times 0.83\text{ nm}$  and  $0.40\text{ nm} \times 0.40\text{ nm}$  square channels along the *b* and *c* directions,  $0.85\text{ nm} \times 0.40\text{ nm}$  “brick-wall” like channel along the *a* direction. Guest water molecules,  $\text{Na}^+$  and  $\text{ClO}_4^-$  ions are encapsulated in the channels of this 3D opening framework. The magnetic measurements reveal it exhibits ferromagnetic interaction. The electrical conductivity measurement reveals it is a semiconductor with active energy of  $0.80\text{ eV}$ . CCDC: 247661.

**Key words:** copper; malonic acid; polymer; self-assembly; semiconductor; ferromagnetic interaction

## 0 Introduction

In recent years, great interest has been focused on the design and synthesis of supramolecular complexes owing to their novel structural motifs and intriguing applications including catalysis, nonlinear op-

tics, sensors, magnetism and molecular recognition<sup>[1,2]</sup>. Up to now a number of new coordination polymeric solids with beautiful architectures and interesting topologies have been reported<sup>[3]</sup>, but a rational synthesis strategy about how to manipulate the assembly of donor and acceptor building blocks to generate de-

收稿日期: 2005-01-17. 收修改稿日期: 2005-03-18。

国家自然科学基金资助项目(No.20171021)。

\*通讯联系人。E-mail: wangzl@nju.edu.cn; Tel: +86-25-83686082

第一作者: 陈 军, 女, 32 岁, 硕士研究生, 讲师; 研究方向: 配位化学。

sired supramolecular architecture is still one of great challenges. Although many efforts have been focused on the construction of extended framework using rigid ‘tecton’ ligands containing O-donor or N-donor to bind metal centers, such as bipyridine, polyaromatic acids and their related species<sup>[4]</sup>, similar researches based on flexible ligands are still very limited<sup>[5]</sup>. When reacting with metal ions, such ligands may show attractive flexibility in the construction of unique frameworks with useful properties.

The investigation of porous solids containing highly mobile alkali metal cations is useful for the development of fast-ion conductors<sup>[6]</sup>, which may have potential applications in areas such as batteries, fuel cells, electrochemical sensors and photocatalysis. On the other hand, the formation of artificial ionic channel structures in the crystalline solid has been reported by a number of groups who aimed to mimic ion transport<sup>[7]</sup>—one of the most essential biological reactions in living systems.

Recently, we have chosen flexible malonic acid as ligand and attempted to explore the synthetic strategies and structure features. In this paper, we will report the synthesis, crystal structure and electrical conductivity characterization of a new 3-D porous architecture, namely  $\text{Na}[\text{Cu}_2(\text{malonate})_2] \cdot (\text{ClO}_4) \cdot (\text{H}_2\text{O})_2$ . In the compound, guest water molecules,  $\text{Na}^+$  and  $\text{ClO}_4^-$  ions are encapsulated in the channels of the neutral opening framework.

## 1 Experimental section

### 1.1 Materials and instrumentation

$\text{Cu}(\text{ClO}_4)_3 \cdot 6\text{H}_2\text{O}$  were synthesized by dissolving  $\text{CuCO}_3 \cdot \text{Cu}(\text{OH})_2$  in an excess amount of perchloric acid. Other starting materials were of reagent grade

and used without further purification. Elemental analysis was performed using a Perkin-Elmer 240c analytical instrument. Conductivity Measurements: The cylindrical pellets of the sample (0.1 cm in thickness and 0.4 cm in diameter) were coated with silver paint on either side. The conductivity measurements were carried out using a standard setup coupled with Agilent 4284A LCR Meter. Variable temperature (1.8~300 K) magnetic susceptibility were measured in the crystalline state on a SQUID MPMS-XL7 at an applied field of 2 kG.

### 1.2 Synthesis of $\text{Na}[\text{Cu}_2(\text{malonate})_2] \cdot (\text{ClO}_4) \cdot (\text{H}_2\text{O})_2$

To an aqueous solution (10 mL) of  $\text{Cu}(\text{ClO}_4)_2 \cdot 6\text{H}_2\text{O}$  (0.371 g, 1 mmol), malonic acid (0.104 g, 1 mmol) was added. After the pH value of the reaction mixture was carefully adjusted to about 6.0 by slow addition of  $0.1 \text{ mol} \cdot \text{L}^{-1}$  NaOH solution. The solution was filtrated to remove the precipitate after a further two hours of stirring and left undisturbed at room temperature. Blue crystals were obtained about a month later. Yield: 0.11 g, 45%. [Found(%): C, 14.80; H, 1.55. Calc(%). for  $\text{C}_6\text{H}_8\text{ClCu}_2\text{NaO}_{14}$ : C, 14.72; H, 1.65].

### 1.3 X-ray crystallography

Intensity data were collected on a Rigaku Mercury CCD area-detector at 293(2) K with Mo  $K\alpha$  radiation ( $\lambda=0.071\,073$  nm). The structure was solved by direct method using SHELXS-97<sup>[8]</sup> and was refined by full-matrix least squares methods using SHELXL-97. Anisotropic displacement parameters were refined for all non-hydrogen atoms. All hydrogen atoms were added geometrically and not refined. Final  $R = \sum (|F_o| - |F_c|) / \sum |F_o|$ ,  $R_w = \{ \sum w[(F_o^2 - F_c^2)^2] / \sum w[(F_o^2)^2] \}^{1/2}$ , with  $w = 1/[\sigma^2(F_o^2) + (aP)^2 + bP]$  [where  $P = (F_o^2 + 2F_c^2)/3$ ,  $a=0.04$ ,  $b=0$ ]. A summary of crystal data and structure refinement for

Table 1 Crystallographic and data collection parameters for the complex

Empirical formula	$\text{C}_6\text{H}_8\text{ClCu}_2\text{NaO}_{14}$	$D_c / (\text{g} \cdot \text{cm}^{-3})$	2.272
Formula weight	489.64	$F(000)$	968
Crystal system	Orthorhombic	Measured reflections	8 170
Space group	$Pnma$	Independent reflections	1 328
$a / \text{nm}$	1.256 5(3)	Observed reflections [ $I > 2\sigma(I)$ ]	1 071
$b / \text{nm}$	1.059 43(2)	$R(\text{int})$	0.065 4
$c / \text{nm}$	1.075 56(14)	Goodness of fit on $F^2$	1.008
Volume / $\text{nm}^3$	1.431 7(4)	$R$	0.041 2
$Z$	4	$wR$	0.078
$\theta$ range for data collection / ( $^\circ$ )	2.70 to 25.02	Max / mean shift in final cycle	0.000 / 0.000
$hkl$ range	-13 to 14, -12 to 12, -12 to 12	Maximum / minimum $\Delta\rho / (\text{e} \cdot \text{nm}^{-3})$	493 / -811

**Table 2** Selected bond lengths (nm) and bond angles ( $^\circ$ ) for the title compound

Cu(1)-O(1)	0.192 1(3)	Cu(2)-O(2)#3	0.200 1(3)	Cu(2)-O(4)	0.197 0(3)
Cu(1)-O(3)	0.191 8(3)				
O(3)#1-Cu(1)-O(3)	86.33(17)	O(3)-Cu(1)-O(1)#1	177.91(12)	O(4)-Cu(2)-O(2)#3	94.03(11)
O(3)#1-Cu(1)-O(1)	177.91(12)	O(1)-Cu(1)-O(1)#1	86.97(18)	O(4)#2-Cu(2)-O(2)#4	94.03(11)
O(3)-Cu(1)-O(1)	93.31(12)	O(4)#2-Cu(2)-O(4)	180	O(4)-Cu(2)-O(2)#4	85.97(11)
O(3)#1-Cu(1)-O(1)#1	93.31(12)	O(4)#2-Cu(2)-O(2)#3	85.97(11)	O(2)#3-Cu(2)-O(2)#4	180

Symmetry transformations used to generate equivalent atoms: #1:  $x, -y+3/2, z$ ; #2:  $-x+2, -y+1, -z+1$ ; #3:  $-x+3/2, -y+1, z+1/2$ ; #4:  $x+1/2, y, -z+1/2$ .

the compound are provided in Table 1. The selected bond lengths and angles are listed in Table 2.

CCDC: 247661.

## 2 Results and discussion

### 2.1 Description of structure

The coordination environment around the Cu (II) centers of the complex is shown in Fig.1. It can be seen from Fig.1 that Cu(1) is four-coordinated and has an O4 donor set which consists of four carboxylate oxygen atoms from two malonic acids. The distance of Cu-O (carboxylate oxygen) is about 0.192 0 nm. To Cu(1), small deviations of bond angles from the idealized square geometry are found for angles O(3)-Cu(1)-O(1A) [ $177.91(12)^\circ$ ], O(3A)-Cu(1)-O(1) [ $177.91(12)^\circ$ ], implying that the  $\text{Cu}^{2+}$  ion has a distorted square planar coordination configuration. It should be noted that at the apical positions, two oxygen atoms (one is from water

molecule and the other is from  $\text{ClO}_4^-$  ion) are weak coordinate to the metal ion. The corresponding separations are 0.263 8(4) and 0.254 4(5) nm respectively. Two malonic acids coordinate to Cu(1) in chelate mode and two six-membered rings are formed. The relevant angle is O(1)-Cu(1)-O(3) [ $93.31(12)^\circ$ ]. Cu(2) is also four-coordinated in a square planar geometry and has an O4 donor set which consists of four carboxylate atoms from four malonic acids. The average distance of Cu-O (carboxylate oxygen) is about 0.198 5 nm, longer than that of Cu(1)-O. There are also two weak coordinated water molecules at the apical positions of Cu(2) with separations of about 0.267 2 nm.

Each malonic acid adopts a  $[3.1_11_21_21_3]$  coordination mode, coordinates to three copper ions. It uses two neighboring carboxylate oxygen atoms (from the two carboxylate groups respectively) to chelate to Cu(1) and the other two spare carboxylate oxygen atoms to coordinate to Cu(2) and Cu(2A) respectively. There are electrovalent bonds between the  $\text{Na}^+$  ion and the surrounding seven oxygen atoms from the carboxylate groups, water molecules and  $\text{ClO}_4^-$ . The Na-O bond distances are in the range of 0.221 0~0.274 3 nm.

Twelve copper atoms and eight ligands were used to form a square  $[\text{Cu}_{14}(\text{malonate})_8]$  subunit, which was used to construct the 3D network. Extension of this subunit through the symmetry equivalent units gives a 3D opening supramolecular framework. Fig.2 shows the two packing diagrams. The compound has 0.98 nm  $\times$  0.83 nm square channels along the  $b$  direction, 0.85 nm  $\times$  0.40 nm “brick-wall” like channels along the  $a$  direction and 0.40 nm  $\times$  0.40 nm square channels viewed along the  $c$  direction. The effective free volume of the square channel is about 0.441 2 nm<sup>3</sup>, comprising 30.8% of the unit cell volume, as calculated by the program PLATON<sup>[9]</sup>. This value is large among

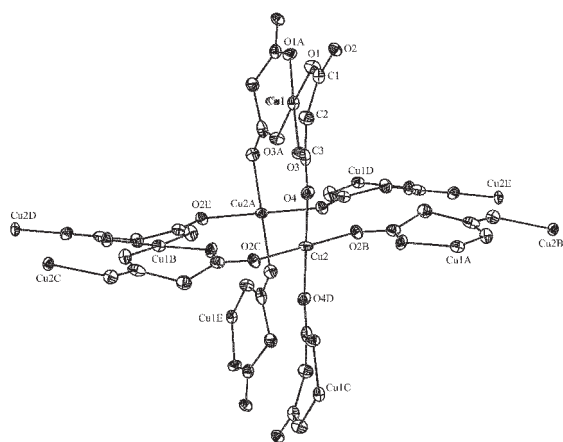


Fig.1 A view of the coordination environment around the Cu(II) centers with the atom numbering scheme, the hydrogen atoms are omitted for clarity (ellipsoids at 30% probability)

Symmetry code (A:  $x, -y+3/2, z$ ; B:  $-x+2, -y+1, -z+1$ ; C:  $-x+3/2, -y+1, z+1/2$ ; D:  $x+1/2, y, -z+1/2$ )

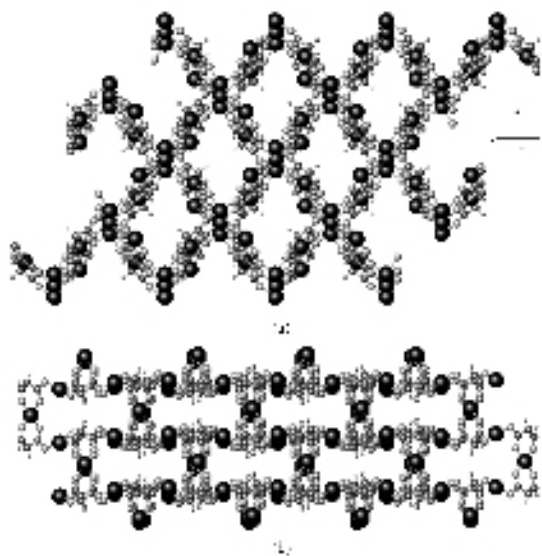


Fig.2 (a) 0.98 nm  $\times$  0.83 nm square channels viewed along the  $b$  direction; (b) 0.85 nm  $\times$  0.40 nm "brick-wall" like channels viewed along the  $a$  direction

The free  $\text{Na}^+$  and  $\text{ClO}_4^-$  ions are omitted for clarity.

the known microporous networks<sup>[10]</sup>. Guest free water molecules,  $\text{Na}^+$  and  $\text{ClO}_4^-$  ions are encapsulated in the large pores.

Previous author have obtained mononuclear, dinuclear and trinuclear compounds through the self-assembly of  $\text{Cu}^{2+}$  and malonic acid ligand<sup>[11]</sup>. We think the reason why we can obtain a 3-D porous architecture may be due to the template role of  $\text{Na}^+$  and  $\text{ClO}_4^-$  ions.

## 2.2 Infrared spectra

Infrared spectra were recorded in the range of 4 000~400  $\text{cm}^{-1}$  as KBr disc. For the free ligand, two strong peaks at 1 700 and 1 400  $\text{cm}^{-1}$  are observed, which may be assigned to  $\nu_{\text{as}}(\text{OCO})$   $\nu_{\text{s}}(\text{OCO})$  of the carboxylate group respectively. But in the complex, the peaks moved to 1 591  $\text{cm}^{-1}$  and 1 369  $\text{cm}^{-1}$  respectively. These frequencies are significantly shifted to lower frequencies by the coordination of malonate to metal ions. In the spectrum of the complex, the 3 522  $\text{cm}^{-1}$  strong and broad band can be assigned to the stretching vibration of the H-O group of water molecule. The presence of  $\text{ClO}_4^-$  group is proved by the strong bands at 1 110, 1 090 and 628  $\text{cm}^{-1}$ .

## 2.3 Electrical conductivity property

Temperature dependent of the electrical conductivity of the complex was determined with powder

sample from grounded crystals. The electrical conductivity of the complex at 253.15 K is  $5.6 \times 10^{-9} \text{ S} \cdot \text{cm}^{-1}$  and increases to  $1.1 \times 10^{-5} \text{ S} \cdot \text{cm}^{-1}$  at 303.15 K, which indicates that it is a semiconductor. The electrical conductivity values as a function of the reciprocal temperature were plotted as  $\ln(\sigma)$  vs  $1000/T$  and shown in Fig.3. The Arrhenius law is given by eq. (1).

$$\sigma = \sigma_0 \exp(E_a / KT) \quad (1)$$

where  $\sigma_0$  is preexponential factor,  $E_a$  is the activation energy for conduction,  $K$  is Boltzmann's constant and  $T$  is the absolute temperature. Using the equation to fit the experimental value gives the activation energy of the polymer is 0.80 eV. We notice several other coordination polymers also show similar semiconducting properties<sup>[12]</sup>. Detailed work on the mechanism of the conductivity of the compound is still in progress.

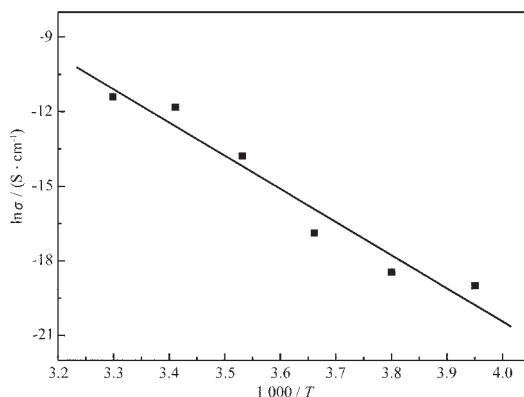


Fig.3 Electrical conductivity values as a function of the reciprocal temperature was plotted as  $\ln(\sigma)$  vs  $1000/T$

## 2.4 Magnetic properties

The magnetic susceptibility of the complex were shown in Fig.4 in the forms  $\chi_M$  and  $\chi_M T$  versus  $T$ . At room temperature,  $\chi_M T$  is 0.91  $\text{emu} \cdot \text{K} \cdot \text{mol}^{-1}$ , which is closed to the spin-only value, 0.83  $\text{emu} \cdot \text{K} \cdot \text{mol}^{-1}$ , based on  $\text{Cu}^{II}_2$  unit ( $S=1/2$  and  $g=2.1$ ). As the temperature decreases,  $\chi_M T$  first increases gradually to 1.1  $\text{emu} \cdot \text{K} \cdot \text{mol}^{-1}$  around 20 K, then abruptly goes up to 1.44  $\text{emu} \cdot \text{K} \cdot \text{mol}^{-1}$  at 1.8 K, indicating the ferromagnetic properties in this complex. The further evidence is from the variable-field magnetization measurements at 1.8 K (Fig.5). The magnetization increases with the increasing field and tends to the saturation (1.87  $N\beta \cdot \text{mol}^{-1}$  at 7 T), but it does not reach the theoretical saturation value of  $2.1 \times 1/2 \times 2 = 2.1 N\beta \cdot \text{mol}^{-1}$  due to a possible Curie temperature lower than 1.8 K. No loop

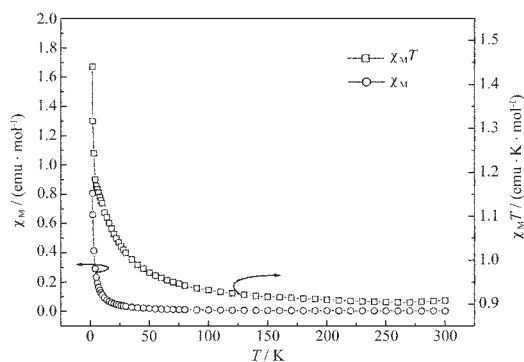


Fig.4 Variable temperature susceptibilities measurements for the complex in the forms  $\chi_M$  (○) and  $\chi_M T$  (□) versus  $T$

The solid lines are the guides for eyes.

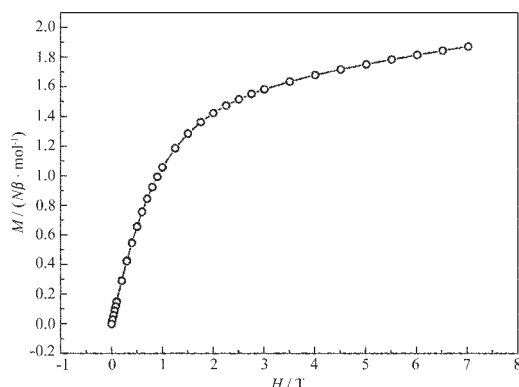
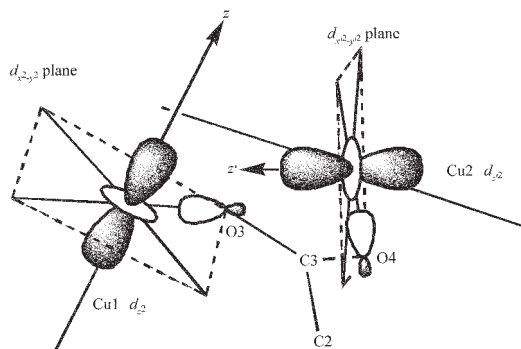


Fig.5 Field dependence of magnetization for the title compound

was observed in M-H measurements and no any signal was determined in AC measurements, indicating no long-range ordering above 1.8 K.

For the 3D structure of the complex, there is no an appropriate model for investigating the magnetic properties in details. However, it is obvious that the carboxylate bridges mediate the ferromagnetic coupling between  $\text{Cu}^{\text{II}}$  ions in this complex. In the complex, malonate coordinates the neighboring two  $\text{Cu}^{\text{II}}$  ions only via  $d_{x^2-y^2}$  orbitals of  $\text{Cu}^{\text{II}}$  ions and the angle of the  $d_{x^2-y^2}$  planes of Cu(1) and Cu(2) is  $113.0^\circ$ . This means that the two orbitals can not effectively overlap by malonate in the spatial orientation of the complex. Equally, the magnetic orbitals,  $d_z$ , of the two  $\text{Cu}^{\text{II}}$  ions located in an elongated octahedral and a distorted octahedral environments, respectively, cannot overlap to form an antiferromagnetic coupling pathway. Namely, the  $d_z$  magnetic orbitals belong to the two  $\text{Cu}^{\text{II}}$  ions are orthogonal each other. Thus, malonate ligands me-

diates the ferromagnetic coupling between  $\text{Cu}^{\text{II}}$  ions in this complex. This bridge factually functions a different magnetic effect from that in the previously reported works [13], although these complexes with syn-anti malonate bridges also show the ferromagnetic properties. In the previously reported works, the  $\text{Cu}^{\text{II}}$  ions are located in the square-based pyramidal environments and the magnetic orbitals are  $d_{x^2-y^2}$ , contrarily, the complex provides  $d_z$  as the magnetic orbital (Scheme 1). So, it exhibits the essential difference with those previously reported in magnetic exchange mechanism.



Scheme 1 Magnetic coupling pathway in the complex

**Acknowledgments:** This research was supported by grants from the National Science Foundation of China.

## References:

- [1] (a) Lehn J M. *Supramolecular Chemistry-Concepts and Perspectives*, VCH: Weinheim, **1995**.  
(b) Yaghi O M, Li H, Davis C, et al. *Acc. Chem. Res.*, **1998**, **31**:474~484
- [2] (a) Byrn M P, Curtis C J, Hsiou Y, et al. in *Solid-State Supramolecular Chemistry: Crystal Engineering, Comprehensive Supramolecular Chemistry* (Eds.: D. D. MacNicol, F. Toda, R. Bishop), Elsevier: Oxford, U. K., **1996**, **6**:715~719  
(b) Würthner F, Sautter A. *Chem. Commun.*, **2000**, **6**:445~446
- [3] (a) Stang P J, Olenyuk B. *Acc. Chem. Res.*, **1997**, **30**:502~518  
(b) Tong M L, Chen H J, Chen X M. *Inorg. Chem.*, **2000**, **39**: 2235~2238  
(c) Dai J C, Hu S M, Wu X T, et al. *New J. Chem.*, **2003**, **27**: 914~918
- [4] (a) Zaworotko M J. *Chem. Commun.*, **2001**, **1**:1~9  
(b) Dai J C, Wu X T, Fu Z Y, et al. *Chem. Commun.*, **2002**, **1**:12~13
- [5] Li J R, Bu X H, Zhang R H. *Inorg. Chem.*, **2004**, **43**:237~244

- [6] Zheng N F, Bu X H, Feng P Y. *Nature*, **2003**,**426**:428~432
- [7] Akutagawa T, Hasegawa T, Nakamura T. *Chem. Eur. J.*, **2001**, **7**:4902~4912
- [8] Sheldrick G M. *SHELXS-97, Program for X-ray Crystal Structure Solution*, University of Göttingen, Göttingen, Germany, **1997**.
- [9] Spek A L. *PLATON, Version 1.62*, University of Utrecht, Utrecht, **1999**.
- [10] Zhang J J, Sheng T L, Hu S M, et al. *Chem. Eur. J.*, **2004**, **10**:3963~3969 and references therein
- [11](a) Lenstra A T H, Kataeva O N. *Acta Crystallogr., Sect. B (Str. Sci.)*, **2001**,**57**:497~506
- (b) Chattopadhyay D, Chattopadhyay S K, Lowe P R, et al. *J. Chem. Soc., Dalton Trans.*, **1993**:913~916
- (c) Naumov P, Ristova M., Soptrajanov B, et al. *Croat. Chem. Acta*, **2002**,**75**:701~711
- [12](a) Zhang J J, Sheng T L, Xia S Q, et al. *Inorg. Chem.*, **2004**, **43**:5472~5478
- (b) Zhang J J, Xia S Q, Sheng T L, et al. *Chem. Commun.*, **2004**,**10**:1186~1187
- [13](a) Ruiz-Pérez C, Sanchiz J, Molina M H, et al. *Inorg. Chem.*, **2000**,**39**:1363~1370
- (b) Konar S, Mukherjee P S, Drew M G B, et al. *Inorg. Chem.*, **2003**,**42**:2545~2552